

Robust Adaptive Control of STATCOMs to Mitigate Inverter-Based-Resource (IBR)-Induced Oscillations

Hui Yuan, Huanhai Xin, Linbin Huang, Huisheng Gao, Jikui Xing, Di Zheng.

Abstract—The interaction among inverter-based resources (IBRs) and power network may cause small-signal stability issues, especially in low short-circuit grids. Besides, the integration of static synchronous compensators (STATCOMs) in a multi-IBR system for voltage support can deteriorate small-signal stability. However, it is still challenging to understand the impact mechanism of STATCOMs on IBR-induced oscillation issues and to design STATCOMs' control for damping these oscillation issues in a multi-IBR system, due to complex system dynamics and varying operating conditions. To tackle these challenges, this paper proposes a novel method to reveal how STATCOMs influence IBR-induced oscillation issues in a multi-IBR system from the viewpoint of grid strength, which can consider varying operating conditions. Based on this proposed method, we find *critical* operating conditions, wherein the system tends to be most unstable; moreover, we demonstrate that robust small-signal stability issues of the multi-IBR system with STATCOMs can be simplified as that of multiple subsystems under *critical* operating conditions, which avoids traversing all operating conditions and establishing system's detailed models. On this basis, an adaptive control-parameter design method is proposed for STATCOMs to ensure system's robust small-signal stability under varying operating conditions. The efficacy of proposed methods is validated by a 39-node test system.

Index Terms—inverter-based resources (IBRs), STATCOMs, small-signal stability, grid strength, adaptive control.

I. INTRODUCTION

The increasing penetration of renewable resources, commonly interfacing with ac grids through power inverters, is changing modern power system dynamics and challenging secure grid operations^{[1],[2]}. Particularly, inverter-based resources (IBRs) with widely-used grid-following controls tracking grid frequency through phase-lock loops (PLLs) may cause sub/sup-synchronous oscillation issues due to strong interaction between fast dynamics of IBRs and grid network, especially in low short-circuit grids^{[3]-[10]}. Besides, in practical wind farms and photovoltaic plants, static synchronous compensator (STATCOM) is commonly required for reactive power compensation. However, STATCOMs can interact with IBRs and even deteriorate IBR-induced oscillation issues^{[11]-[12]}. For instance, in 2015, a sub-synchronous resonance event was recorded in wind farms with STATCOMs in Hami, China^[11].

STATCOMs have complex interaction with IBRs through power network, especially considering multiple STATCOMs

and IBRs, and varying operating conditions. This makes it hard to understand how STATCOMs influence IBR-induced oscillation issues. To understand STATCOMs' impact mechanism, Ref. [11] established the sequence impedance of a wind farm with a STATCOM and evaluated the damping provided by the STATCOM. The impedance-based analysis method commonly used Nyquist stability criterion for small-signal stability analysis, which is based on reduced SISO transfer function of the system with the assumption that it has no right-half-plane pole. However, this assumption is not always satisfied^[13]. To avoid this issue, Ref. [12] proposed a generalized short-circuit ratio (gSCR)-based method from the viewpoint of grid strength to reveal how the interaction among STATCOMs and IBRs impacts small-signal stability in a multi-IBR system with STATCOMs under rated operating condition. It is noteworthy that varying operating conditions change system's equilibrium and thus influence small-signal stability. However, it is still unknown how varying operating conditions influence the interaction among STATCOMs and IBRs, and the system's small-signal stability.

To suppress IBR-induced oscillation issues, many works proposed improved control strategies, which can be divided into two categories: control design of IBRs^[14] and control design of additional devices (e.g., STATCOMs^{[11],[15]}). For instance, Ref. [14] proposed a PLL-reshaping method to improve small-signal stability of a single-IBR infinite-bus system. However, IBRs are commonly packaged and thus it is hard to modify IBR's control in practical operations. In comparison, STATCOMs are "white-boxed" models and thus it is more convenient to modify STATCOMs' control. For instance, Ref. [11] proposed an intelligent parameter design method for STATCOMs to mitigate resonance in wind farms, which is based on gain margin and phase margin of the system's SISO transfer function. However, this method may be ineffective if the obtained SISO transfer function has right-half-plane poles. Ref. [15] proposed an enhancing-grid stiffness control strategy of STATCOMs, which shapes STATCOMs' impedance as inductances and improves the stability by increasing grid strength or short-circuit ratio (SCR). However, these previous works mainly focused on one certain operating condition, which cannot ensure robust small-signal stability of the system under varying operating conditions.

To robustly mitigate IBR-induced oscillations under varying operating conditions, this paper proposes an adaptive control parameter design method for STATCOMs. We firstly propose a grid-strength-based method to analyze small-signal stability of the multi-IBR system with STATCOMs under varying operating conditions, which was the extension of our previous work for the multi-IBR system with STATCOMs under rated

H. Yuan, H. Xin, H. Gao, and J. Xing are with college of electrical engineering, Zhejiang university, Hangzhou 310027, China (Email: Yuan_Hui@zju.edu.cn; xinhh@zju.edu.cn; gaohuisheng@zju.edu.cn);

L. Huang is with department of information technology and electrical engineering, ETH Zürich, 8092 Zürich, Switzerland (e-mail: linhuang@ethz.ch);

D. Zheng is with College of Mechanical and Electrical Engineering, China Jiliang University, Hangzhou 310018, China (e-mail: di.zh@cjlu.edu.cn).

operating condition^[12]. Based on the proposed method, the impact mechanism of STATCOMs on IBR-induced oscillation issues is revealed from the viewpoint of grid strength. Moreover, based on the proposed method, we find *critical* operating conditions, wherein the system tends to be most unstable; and we demonstrate that the small-signal stability of the original system is bounded by multiple subsystems. On these bases, we simplify robust small-signal stability issues of the multi-IBR system with STATCOMs under varying operating conditions as that of multiple subsystems under *critical* operating conditions, which avoids traversing all operating conditions and establishing detailed system models. Moreover, an adaptive control parameter design method for STATCOMs is proposed to ensure robust small-signal stability of established multiple subsystems under *critical* operating conditions, which is also robustly effective for the original system under varying operating conditions. Besides, the proposed control method can consider the scenario that IBRs are “black-boxed” models. The main contributions of this paper can be summarized as:

1) A grid-strength-based method is proposed to evaluate small-signal stability of the multi-IBR system with STATCOMs under varying operating conditions. On this basis, we reveal impact mechanism of STATCOMs on IBR-induced oscillation issues from the viewpoint of grid strength.

2) Based on the grid-strength-based method, the robust small-signal stability issues of a multi-IBR system with STATCOMs under varying operating conditions are simplified as multiple subsystems under *critical* operating conditions. This can avoid traversing all operating conditions and establishing system’s detailed models.

3) Based on the H_∞ control theory^[16], an adaptive control parameter design method is proposed for STATCOMs to ensure robust small-signal stability of established multiple subsystems under *critical* operating conditions. It is verified that the proposed control method can also ensure robust small-signal stability of the original system under varying operating conditions, even that the IBRs are “black-box” models.

The rest of this paper is organized as follows. Section II introduces the dynamic model of the multi-IBR system with STATCOMs under varying operating conditions and focused issues. In section III, a grid-strength-based method is proposed to reveal the impact mechanism of STATCOMs on IBR-induced oscillation issues considering varying operating conditions. Section IV simplifies robust small-signal stability issues of the multi-IBR system with STATCOMs under varying operating conditions. Section V proposes an adaptive control parameter design method for STATCOMs. In Section VI, the efficacy of proposed methods is demonstrated by eigenvalue analysis and time-domain simulations on a 39-node system. In section VII, the conclusions are drawn.

II. SYSTEM MODELING AND PROBLEM DESCRIPTION

Let us consider a multi-IBR system with k STATCOMs as shown in Fig. 1, where nodes $1 \sim n$ are connected to IBRs, node $n+m+1$ is connected to external grids (simplified as ideal voltage source); remaining nodes are passive nodes. Since in

practice STATCOMs are not directly connected to IBRs’ terminal nodes, we assume that STATCOM1~STATCOM k are connected to passive nodes $n+1 \sim n+k$. To simplify the analysis, we assume that: STATCOMs are all applied with ac-voltage control (AVC) and control parameters of STATCOMs are identical; AVC of STATCOMs is not saturated, i.e., reactive current reference I_{qsref} is in range of $[-1,1]$; IBRs’ terminal voltage remains nearly at 1 p.u. due to STATCOMs’ voltage support; we mainly consider the changes of IBRs’ active power outputs and STATCOMs’ reactive current outputs under varying operating conditions, but network parameters, and control parameters of IBRs and STATCOMs are fixed.

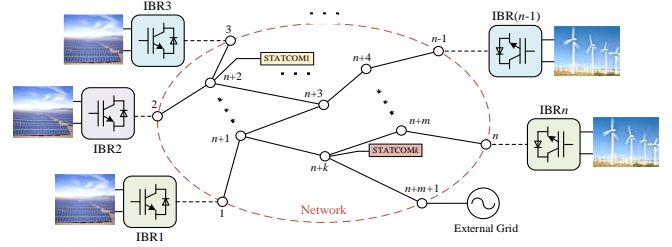


Fig. 1 One-line diagram of a typical multi-IBR system with STATCOMs.

When operating under non-rated conditions, the closed-loop characteristic equation of the multi-IBR system with STATCOMs can be given as (1) for small-signal stability analysis:

$$\det(\mathbf{Y}_{Gm}(s) + \mathbf{Y}_{Nm}(s)) = 0 \quad (1)$$

$$\mathbf{Y}_{Gm}(s) = \begin{bmatrix} \text{diag}(\mathbf{Y}'_{IBRi}(s)) & \\ & \text{diag}(\mathbf{Y}'_{STAJj}(s)) \end{bmatrix} \quad (2)$$

$$\begin{cases} \mathbf{Y}'_{IBRi}(s) = P_{ei} \mathbf{Y}_{IBRi}(s), & i = 1, \dots, n \\ \mathbf{Y}'_{STAJj}(s) = S_{Bsj} \mathbf{Y}_{STAJj}(s), & j = 1, \dots, k \end{cases} \quad (3)$$

$$\mathbf{Y}_{STAJj}(s) = \begin{bmatrix} Y_{11}(s) & I_{qsj} Y_{12}(s) \\ Y_{21}(s) & Y_{22}(s) \end{bmatrix} \quad (4)$$

$$\mathbf{Y}_{Nm}(s) = \mathbf{B}_{red} \otimes \boldsymbol{\gamma}(s) = \begin{bmatrix} \mathbf{B}_{11} & \mathbf{B}_{12} \\ \mathbf{B}_{21} & \mathbf{B}_{22} \end{bmatrix} \otimes \boldsymbol{\gamma}(s) \quad (5)$$

$$\boldsymbol{\gamma}(s) = \frac{1}{(s + \tau)^2 / \omega_0 + \omega_0} \begin{bmatrix} (s + \tau) & \omega_0 \\ -\omega_0 & (s + \tau) \end{bmatrix} \quad (6)$$

where $\mathbf{Y}_{Gm}(s)$ and $\mathbf{Y}_{Nm}(s)$ denote admittance matrices of devices and network, wherein the similar derivation refers to Ref. [12]; $\text{diag}()$ denotes a diagonal block matrix; $\mathbf{Y}'_{IBRi}(s)$ and $\mathbf{Y}'_{STAJj}(s)$ are admittance matrices of $IBRi$ and $STATCOMj$, of which the detailed derivation refers to Ref. [17] and [18]; P_{ei} and S_{Bsj} are active power output of $IBRi$ and rated capacity of $STATCOMj$; I_{qsj} is reactive current output of $STATCOMj$; $Y_{11}(s)$, $Y_{12}(s)$, $Y_{21}(s)$, $Y_{22}(s)$ are elements of $\mathbf{Y}_{STAJj}(s)$, which has no relation with I_{qsj} ; $\mathbf{Y}_{IBRi}(s)$ and $\mathbf{Y}_{STAJj}(s)$ are admittance matrices of $IBRi$ and $STATCOMj$ normalized at their rated capacities; $\mathbf{B}_{red} \in \mathbf{R}^{(n+k) \times (n+k)}$ is network node-reduced susceptance matrix containing IBR nodes and STATCOM nodes; $\mathbf{B}_{11} \in \mathbf{R}^{n \times n}$, $\mathbf{B}_{12} \in \mathbf{R}^{n \times k}$, $\mathbf{B}_{21} \in \mathbf{R}^{k \times n}$, $\mathbf{B}_{22} \in \mathbf{R}^{k \times k}$ are submatrices of \mathbf{B}_{red} ; $\tau = R/L$ denotes line ratio of resistor (R) to inductance (L). We assume that all network lines have same ratio τ ; ω_0 is rated synchronous frequency.

By submitting (2) and (5) into (1), the closed-loop characteristic equation (1) can be written as:

$$\det \left(\begin{bmatrix} \text{diag}(P_{ei} \mathbf{Y}_{IBRi}(s)) \\ \text{diag}(S_{Bsj} \mathbf{Y}_{STAJ}(s)) \end{bmatrix} + \mathbf{B}_{red} \otimes \boldsymbol{\gamma}(s) \right) = 0 \quad (7)$$

We can see from (7) that IBRs interact with STATCOMs through the network, which may cause small-signal stability issues, especially in weak grids. To this end, this paper mainly focuses on addressing two issues:

- 1) How to reveal impact mechanism of STATCOMs on IBR-induced oscillation issues under varying operating conditions?
- 2) How to design control of STATCOMs to ensure system's robust stability under varying operating conditions?

For *issue 1*, we can see from (7) that it is challenging to directly solve characteristic equation (7) for small-signal stability analysis, because of complex interactions among IBRs and STATCOMs through the network, especially considering varying operating conditions. To deal with this issue, a grid-strength-based method will be proposed in Section III. For *issue 2*, an adaptive parameter design method for STATCOMs will be proposed in Section IV.

III. IMPACT MECHANISM OF STATCOMS ON IBR-INDUCED OSCILLATION ISSUES UNDER VARYING OPERATING CONDITIONS

A. Proposed Grid-Strength-Based Method

In our previous work^[12], we proposed a generalized short circuit ratio (gSCR)-based method to evaluate small-signal stability of a multi-IBR system with STATCOMs under rated operating condition. To be specific, we convert the multi-IBR system with STATCOMs into an equivalent homogeneous system for small-signal stability analysis. The equivalent homogeneous system can be furtherly decoupled into n independent subsystems for small-signal stability analysis, wherein these subsystems have the same equivalent device but different SCRs. Due to this, the small-signal stability of the equivalent homogeneous system (or the original system) can be represented by the *critical* subsystem with smallest SCR, (named as gSCR). The expression of gSCR is given as:

$$gSCR = \lambda_{\min} \{ \mathbf{S}_B^{-1} \mathbf{B}_{redn} \}, \mathbf{S}_B = \text{diag} \{ S_{Bi} \}, \mathbf{B}_{redn} = \mathbf{B}_{11} - \mathbf{B}_{12} \mathbf{B}_{22}^{-1} \mathbf{B}_{21} \quad (8)$$

where $\lambda_{\min} \{ \}$ denotes smallest eigenvalue of a matrix; \mathbf{S}_B is a diagonal matrix, wherein diagonal element S_{Bi} is rated capacity of IBR i ; \mathbf{B}_{11} , \mathbf{B}_{12} , \mathbf{B}_{21} and \mathbf{B}_{22} refer to (5).

When control parameters of IBRs and STATCOMs are given, gSCR can evaluate small-signal stability margin of the multi-IBR system with STATCOMs under rated operating condition. The characteristic equation of the multi-IBR system with STATCOMs under rated operating condition is given as:

$$\det \left(\begin{bmatrix} \text{diag}(S_{Bi} \mathbf{Y}_{IBRi}(s)) \\ \text{diag}(S_{Bsj} \mathbf{Y}_{STAJ}(s)) \end{bmatrix} + \mathbf{B}_{red} \otimes \boldsymbol{\gamma}(s) \right) = 0 \quad (9)$$

We can see from (7) and (9) that the multi-IBR system with STATCOMs under non-rated operating conditions has a similar characteristic equation as the system under rated operating condition. Therefore, referring to [12], the multi-IBR system with STATCOMs under non-rated operating conditions can also be represented by an equivalent homogeneous system

and its decoupled *critical* subsystem for small-signal stability analysis, as shown in Fig. 2(a). According to Ref. [12], the characteristic equation of the *critical* subsystem is given as:

$$\det(\mathbf{C}_1(s)) = \det(\bar{\mathbf{Y}}_s(s) \boldsymbol{\gamma}^{-1}(s) + \lambda_1 \mathbf{I}_1) = 0, \lambda_1 = \lambda_{\min} \{ \mathbf{P}_e^{-1} \mathbf{B}_{redn} \} \quad (10)$$

$$\bar{\mathbf{Y}}_s(s) = \bar{\mathbf{Y}}_{IBR}(s) + \bar{\mathbf{Y}}_{STA}(s) \quad (11)$$

$$\bar{\mathbf{Y}}_{IBR}(s) = \sum_{i=1}^n p_{1i} \mathbf{Y}_{IBRi}(s), \bar{\mathbf{Y}}_{STA}(s) = \sum_{j=1}^k p_{2j} \mathbf{Y}_{STAJ}(s) \quad (12)$$

$$p_{1i} = v_{1i} u_{1i}, p_{2j} = S_{Bsj} \bar{\mathbf{u}}_1^T \begin{bmatrix} \mathbf{P}_e^{-1} \\ \mathbf{I}_k \end{bmatrix} \mathbf{E}_{sj} \bar{\mathbf{v}}_1 \quad (13)$$

$$\bar{\mathbf{u}}_1^T = [\mathbf{u}_1^T \quad -\mathbf{u}_1^T \mathbf{P}_e^{-1} \mathbf{B}_{12} \mathbf{B}_{22}^{-1}], \bar{\mathbf{v}}_1 = \begin{bmatrix} \mathbf{v}_1 \\ -\mathbf{B}_{22}^{-1} \mathbf{B}_{21} \mathbf{v}_1 \end{bmatrix} \quad (14)$$

where $\mathbf{C}_1(s)$ is closed-loop transfer function matrix; $\bar{\mathbf{Y}}_s(s)$ is device's dynamics, which is weighted sum of all IBRs and STATCOMs; $\mathbf{P}_e = \text{diag}(P_{ei})$ is a diagonal matrix, wherein the diagonal element P_{ei} is active power output of IBR i ; p_{1i} ($i=1, \dots, n$) and p_{2j} ($j=1, \dots, k$) are participation factors; u_{1i} and v_{1i} are i th elements of \mathbf{u}_1^T and \mathbf{v}_1 ; \mathbf{u}_1^T and \mathbf{v}_1 are normalized left and right eigenvectors of smallest eigenvalue λ_1 for $\mathbf{P}_e^{-1} \mathbf{B}_{redn}$; \mathbf{E}_{sj} is a square matrix representing location of STATCOM j , wherein only $(n+j)$ th diagonal element is one and the other elements are zero. $\bar{\mathbf{Y}}_{STA}(s)$ is rewritten as (15) under the assumption that STATCOMs have same control parameters:

$$\bar{\mathbf{Y}}_{STA}(s) = p_{\Sigma} \bar{\mathbf{Y}}_{STA1}(s), \bar{\mathbf{Y}}_{STA1}(s) = \begin{bmatrix} Y_{11}(s) & I_{q\Sigma} \tilde{Y}_{12}(s) \\ Y_{21}(s) & Y_{22}(s) \end{bmatrix} \quad (15)$$

$$p_{\Sigma} = \sum_{j=1}^k p_{2j} \cdot I_{q\Sigma} = \sum_{j=1}^k p_{2j} I_{qsj} / p_{\Sigma} \quad (16)$$

We can see from (15) and (4) that $\bar{\mathbf{Y}}_{STA}(s)$ can be considered as the dynamic of a STATCOM, where p_{Σ} and $I_{q\Sigma}$ represent capacity and reactive current output. Moreover, since $p_{2j} \geq 0$ and I_{qsj} is in range of $[-1, 1]$, $I_{q\Sigma}$ is in range of $[-1, 1]$. Thus, the dynamics of the device $\bar{\mathbf{Y}}_s(s)$ in (11) can be considered as the weighted sum of IBRs and a STATCOM as shown in Fig. 2(a).

Referring to (8) and (10), we can see that the gSCR and λ_1 have similar forms. In other words, the gSCR can be extended to evaluate small-signal stability of the multi-IBR system with STATCOMs under non-rated operating conditions, when control parameters of IBRs and STATCOMs are given. The difference is that the gSCR is minimal eigenvalue of $\mathbf{P}_e^{-1} \mathbf{B}_{redn}$ for varying operating conditions, i.e.,

$$gSCR = \lambda_{\min} \{ \mathbf{P}_e^{-1} \mathbf{B}_{redn} \} \quad (17)$$

Eqn. (17) can also consider rated operating condition. In this case, IBR i 's active power output is equal to the rated capacity (i.e., S_{Bi}), and thus (17) is equivalent to (8).

The *critical* gSCR (i.e., $CgSCR$) is given as, which represents that the system is *critically* stable:

$$CgSCR = \arg \left\{ \det(\bar{\mathbf{Y}}_s(s_c) \boldsymbol{\gamma}^{-1}(s_c) + gSCR \cdot \mathbf{I}_1) \right\} = 0 \quad (18)$$

where $\arg \{ \}$ denotes the eigenvalue calculation of $CgSCR$; $s_c = j\omega_c$ is dominant eigenvalues of *critical* subsystem in (10), which is located at the imaginary axis in complex plane; ω_c is oscillation frequency.

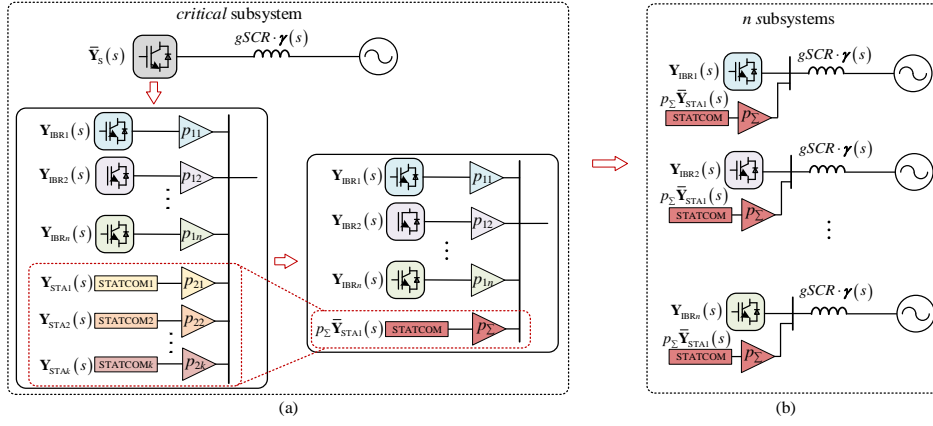


Fig. 2 (a) *critical* subsystem representing small-signal stability of the multi-IBR system with STATCOMs under varying operating conditions; (b) n subsystems that encircles the small-signal stability of the *critical* subsystem as introduced in Section IV.B.

Based on the $gSCR$ and $CgSCR$, we can evaluate small-signal stability of the multi-IBR system with STATCOMs under varying operating conditions from the viewpoint of grid strength. That is, if $gSCR > CgSCR$, the system is stable; the larger the $(gSCR - CgSCR)$ is, the more stable the system is; otherwise, if $gSCR < CgSCR$, the system is unstable.

B. Analysis of STATCOMs' Impact on Small-Signal Stability

As discussed in the above subsection, the multi-IBR system with STATCOMs under varying operating conditions can be represented by the *critical* subsystem (10) for small-signal stability analysis, which considers the change of IBRs' active power outputs P_{ei} , ($i=1, \dots, n$) and STATCOMs' reactive current outputs I_{qsj} , ($j=1, \dots, k$). Moreover, when control parameters of IBRs and STATCOMs are given, the grid-strength indicator, (i.e., $gSCR$) can evaluate small-signal stability margin of the *critical* subsystem (or the original system) under varying operating conditions. Based on the *critical* subsystem and grid-strength indicator, the impact mechanism of STATCOMs on the system stability under varying operating conditions can be described as follows:

1) The connection of STATCOMs has no impact on $gSCR$, but has an impact on $CgSCR$. This is because the $gSCR$ in the *critical* subsystem is that of the multi-IBR system without STATCOMs as shown in (17), but the calculation of $CgSCR$ is related with the dynamics of STATCOMs as shown in (18).

2) Whether STATCOMs increase or decrease $CgSCR$ is uncertain, which depends on the dynamics of STATCOMs including control parameters and reactive current outputs I_{qsj} . The detailed discussion refers to Section VI. Besides, when STATCOMs decrease $CgSCR$ with fixed $gSCR$, the system becomes more stable; otherwise, if STATCOMs increase $CgSCR$ with fixed $gSCR$, the system tends to be unstable. This is because the $(gSCR - CgSCR)$ represents the system's stability margin, and that the larger $(gSCR - CgSCR)$ is, the system is more stable as discussed in the above subsection.

3) Participation factor p_{2j} reflects relative degree of the impact of STATCOM j on $CgSCR$ (or system's stability). We can see from (11), (12) and (18) that the larger p_{2j} is, the larger the impact of STATCOM j on $CgSCR$ is.

4) The decrease of IBRs' active power outputs P_{ei} , ($i=1, \dots, n$) increases participation factor p_{Σ} in (16) and thus increases

relative degree of STATCOMs' impact on $CgSCR$. To be specific, since STATCOMs are commonly connected near IBRs, we approximately consider that STATCOMs are connected to IBR nodes. Due to this, p_{Σ} in (16) is written as

$$p_{\Sigma} = \sum_{i=1}^n \frac{S_{Bsi}}{P_{ei}} p_{li} \quad (19)$$

where S_{Bsi} , ($i=1, \dots, n$) are capacities of STATCOMs, and satisfies $S_{Bsi} \geq 0$, wherein $S_{Bsi} = 0$ means there is no STATCOMs near the node of IBR i ;

Since participation factor p_{li} satisfies $0 < p_{li} < 1$ and $\sum_{i=1}^n p_{li} = 1$, we can conclude from (19) that the decrease of IBRs' active power outputs P_{ei} , ($i=1, \dots, n$) commonly increase p_{Σ} . We mention that the decrease of P_{ei} not only influences $CgSCR$, but also increases $gSCR$. This is because the sensitivity of $gSCR$ for IBRs' active power outputs P_{ei} , ($i=1, \dots, n$) is negative^[19].

5) The decrease of STATCOMs' reactive current outputs I_{qsj} , ($j=1, \dots, k$) only influences $CgSCR$, but has no impact on $gSCR$. As shown in (15) and (16), the change of I_{qsj} , ($j=1, \dots, k$) mainly influences STATCOM's dynamics $\bar{Y}_{STATi}(s)$ and thus influences $CgSCR$. Besides, referring to the above 1), we can conclude that I_{qsj} , ($j=1, \dots, k$) have no impact on $gSCR$. Moreover, it is noteworthy that whether the increase of STATCOMs' reactive current outputs I_{qsj} increases or decreases $CgSCR$ is uncertain, which depends on STATCOMs' dynamics. This will be discussed in Section VI.

IV. SIMPLIFYING ROBUST SMALL-SIGNAL STABILITY ISSUE OF MULTI-IBR SYSTEM WITH STATCOMS UNDER VARYING OPERATING CONDITIONS

In this section, we will first discuss *critical* operating conditions that the system tends to be most unstable. Then, we will furtherly demonstrate that small-signal stability of the *critical* subsystem (representing stability of the original system as discussed in Section III.A) is bounded by that of n subsystems. On these bases, the robust small-signal stability issue of the multi-IBR system with STATCOMs under varying operating conditions can be simplified as that of multiple subsystems under *critical* operating conditions, which will be used in Section V.

A. Discussion of Critical Operating Conditions

When the operating condition changes, so do IBRs' active power outputs P_{ei} , ($i=1, \dots, n$) and STATCOMs' reactive currents outputs I_{qsj} , ($j=1, \dots, k$). According to 3)~5) in Section III.B, we can see that: the decrease of P_{ei} increases p_Σ and gSCR; I_{qsj} only impacts CgSCR but has no impact on gSCR; besides, the impact of I_{qsj} on CgSCR is uncertain, which depends on STATCOMs' dynamics. On these bases, we give a proposition about *critical* operating conditions.

Proposition 1: If STATCOMs decrease CgSCR, then the *critical* operating conditions are that all IBRs output rated active power (i.e., S_{Bi} , $i=1, \dots, n$) with STATCOMs' reactive current outputs I_{qsj} in range of $[-1, 1]$.

Proof: When STATCOMs decrease CgSCR, the decrease of IBRs' active power outputs causes the decrease of CgSCR due to that p_Σ increases. Besides, since the decrease of IBRs' active power output increases gSCR, (gSCR-CgSCR) becomes larger (i.e., the system becomes more stable) with the decrease of IBRs' active power outputs. That is, if the connection of STATCOMs decrease CgSCR, the *critical* subsystem tends to be most unstable under *critical* operating conditions. The proof is concluded ■.

In other words, *critical* operating conditions can be considered as that $gSCR = \lambda_{\min} \{ \mathbf{S}_B^{-1} \mathbf{B}_{redn} \}$ in (8) and $I_{q\sigma}$ in range of $[-1, 1]$ for the *critical* subsystem with the pre-condition that STATCOMs decrease CgSCR. Note that this pre-condition can be satisfied by the proposed control method in Section V.

B. Multi-Subsystem Encircling Stability of Critical Subsystem

The small-signal stability of the multi-IBR system with STATCOMs under varying operating conditions is bounded by the dynamics of IBRs and STATCOMs. To analyze small-signal stability of the multi-IBR system with STATCOMs, we define n equivalent subsystems as shown in Fig. 2(b). These n equivalent subsystems have different devices' dynamics, but the same gSCR. In each subsystem, the devices include a IBR in the original system and a STATCOM $\bar{\mathbf{Y}}_{STA}(s)$ in (15). These two devices are parallel in each subsystem as shown in Fig. 2 (b). Besides, the small-signal stability margin of these n subsystems is ranked in the order from smallest to largest, i.e., subsystem_{1,1}, subsystem_{1,2}, ..., and subsystem_{1,n}.

We can see from Fig. 2 (a) that the participation factor p_{1i} ($i=1, \dots, n$) determines the stability of the *critical* subsystem with given gSCR and dynamics of IBRs and STATCOMs. That is, if the participation factor p_{1i} of the IBR's dynamic (same as that of the subsystem_{1,1}) is larger, the *critical* subsystem will tend to be unstable; if the participation factor p_{1i} of the IBR's dynamic (same as that of the subsystem_{1,n}) is larger, the *critical* subsystem will be more stable. Since the participation factor p_{1i} ($i=1, \dots, n$) satisfy $0 < p_{1i} < 1$ ($i=1, \dots, n$), the extreme cases for the *critical* subsystem with given gSCR and dynamics of IBRs and STATCOMs are that: 1) when participation factor p_{1i} of IBR's dynamic (same as that of subsystem_{1,1}) is one and the other p_{1i} are all zero (i.e., subsystem_{1,1}), the *critical* subsystem is most unstable; 2) when p_{1i} of IBR's dynamic (same as that of

subsystem_{1,n}) is one and the other p_{1i} are all zero (i.e., subsystem_{1,n}), the *critical* subsystem is most stable.

As a result, the small-signal stability of the *critical* subsystem (or the multi-IBR system with STATCOMs) is bounded by subsystem_{1,1} and subsystem_{1,n}, which will be illustrated in Section VI. Besides, since the system tends to be most unstable under *critical* operating conditions as discussed in the above subsection, we can simplify the robust small-signal stability issue of the multi-IBR system with STATCOMs under varying operating conditions as that of subsystem_{1,1}~subsystem_{1,n} under *critical* operating conditions.

V. ADAPTIVE PARAMETER DESIGN OF STATCOMS UNDER VARYING OPERATING CONDITIONS

As discussed in Section IV, the control design issue of the multi-IBR system with STATCOMs for robust small-signal stability under varying operating conditions can be simplified as that of subsystem_{1,1}~subsystem_{1,n} under *critical* operating conditions. Besides, since IBRs are commonly "black-boxed" and thus it is hard to modify IBRs' control strategies in practical operations, we intend to modify STATCOMs' control strategies, which is more convenient. In this section, an adaptive control parameter design method for STATCOMs is proposed to ensure robust small-signal stability of subsystem_{1,1}~subsystem_{1,n} under *critical* operating conditions.

A. Adaptive Control Parameter Design Method for STATCOMs

\mathcal{H}_∞ -synthesis design is an efficient way to ensure the robust small-signal stability, which will be used for adaptive control-parameter design of STATCOMs. For brevity, we omit the detailed introduction of \mathcal{H}_∞ -synthesis design, which can refer to Ref. [16]. Based on \mathcal{H}_∞ -synthesis method and the analysis in Section IV, the adaptive control parameter design problem of STATCOMs can be described as the simultaneous stabilization problem of subsystem_{1,1}~subsystem_{1,n} under *critical* operating conditions or a min-max optimization problem:

$$\min_{\mathbf{K}} \max_{\substack{i=1, \dots, n, I_{q\sigma} \in [-1, 1] \\ gSCR = \lambda_{\min}(\mathbf{S}_B^{-1} \mathbf{B}_{redn})}} \left\| \mathbf{C}_i (s\mathbf{I} - (\mathbf{A}_i + \mathbf{B}_i \mathbf{K} \mathbf{C}_i))^{-1} \mathbf{B}_i \right\|_\infty \quad (20)$$

where $\|\cdot\|_\infty$ is infinite norm; $\mathbf{C}_i (s\mathbf{I} - (\mathbf{A}_i + \mathbf{B}_i \mathbf{K} \mathbf{C}_i))^{-1} \mathbf{B}_i$ is closed-loop transfer function matrix of subsystem_{1,i} under *critical* operating conditions; \mathbf{A}_i , \mathbf{B}_i , \mathbf{C}_i are parameter matrices of open-loop state-space model of subsystem_{1,i}, described as:

$$\text{subsystem}_{1,i} : \begin{cases} \dot{\mathbf{x}}_i = \mathbf{A}_i \mathbf{x}_i + \mathbf{B}_i \mathbf{u}_i \\ \mathbf{y}_i = \mathbf{C}_i \mathbf{x}_i \end{cases} \quad (21)$$

where \mathbf{x}_i , \mathbf{y}_i , and \mathbf{u}_i are vectors of state variables, algebraic variables, and input variables. Note that if IBRs are "black-boxed", parameter matrices \mathbf{A}_i , \mathbf{B}_i and \mathbf{C}_i can be obtained by identifying internal dynamics through rational approximation based on frequency scan^[20]. \mathbf{K} in (20) represents the \mathcal{H}_∞ -controller in STATCOMs, which can be a transfer function matrix related with "s", or a static gain matrix. To simplify the difficulty of adaptive parameter control design of STATCOMs, we do not change the original control structure of STATCOMs, and choose proportional-integral (PI) parameters in AVC and

PLL of STATCOMs as elements in \mathbf{K} . That is, matrix \mathbf{K} can be expressed as:

$$\mathbf{u}_i = \mathbf{K}\mathbf{y}_i, \mathbf{K} = \begin{bmatrix} k_{acps} & k_{acis} & 0 & 0 \\ 0 & 0 & k_{plps} & k_{pllis} \end{bmatrix} \quad (22)$$

where $\mathbf{y}_i = [U_{qsi}, x_{1si}, (U_{si-1}), x_{2si}]^T$, wherein U_{qsi} and U_{si} are q -axis component and amplitude of STATCOM's terminal voltage in subsystem $_{1,i}$; x_{1i} and x_{2i} are the integrations of U_{qsi} and (U_{si-1}) ; $\mathbf{u}_i = [\omega_{pllis}, I_{qrefsi}]^T$, wherein ω_{pllis} is PLL's frequency output, and I_{qrefsi} is q -axis current reference; k_{acps} and k_{acis} are PI parameters in AVC; k_{plps} and k_{pllis} are PI parameters in PLL.

The optimization problem (20) is a pure-stabilization \mathcal{H}_∞ -synthesis problem, of which the necessary and sufficient condition for system's robust small-signal stability is that the objective function in (20) is finite^[16]. Besides, if the objective function in (20) is smaller, the obtained control parameters of STATCOMs can improve system's stability better. However, the range of STATCOM's reactive current output $I_{q\Delta}$ (i.e., $[-1, 1]$) is large in *critical* operating conditions. Due to this, the optimization problem (20) may have no solutions, which will be discussed in Section VI. To deal with this issue, we divide *critical* operating conditions as m sub-conditions. In these sub-conditions, $gSCR = \lambda_{\min}\{\mathbf{S}_B^{-1}\mathbf{B}_{redn}\}$ and $I_{q\Delta}$ is in m intervals, i.e., $[-1, -1+2/m], [-1+2/m, -1+4/m], \dots, [-1+2(m-1)/m, 1]$. For each sub-condition, we establish the corresponding optimization problem (20) and obtain corresponding controller \mathbf{K}_i in (22) to ensure robust small-signal stability of the n subsystems.

In other words, to ensure robust small-signal stability of the multi-IBR system with STATCOMs under varying operating conditions, we firstly obtain a set of controllers $\{\mathbf{K}_1, \dots, \mathbf{K}_m\}$ for STATCOMs by off-line solving established m optimization problems (20), and then on-line adaptively choose proper controller \mathbf{K}_i according to real-time STATCOMs' reactive current outputs and IBRs' active power outputs. Note that by experiment we find that the obtained optimal controller \mathbf{K}_i can ensure to decrease CgSCR of the *critical* subsystem under *critical* operating conditions; besides, if m is larger, \mathbf{K}_i can cause a larger decrease of CgSCR (or improve the system's stability better); but if m is too large, it will cause a high demand of real-time communication and computation for $I_{q\Delta}$; if m is too small or even equal to 1, the optimization problem (20) may have no solutions, which will be illustrated in Section VI. Thus, m should be properly chosen to balance control performance and economical cost.

B. Implementation Procedure of Proposed Control Method

As discussed above, the proposed adaptive control parameter design method for STATCOMs in the multi-IBR system with STATCOMs under varying operating conditions mainly includes two parts: 1) Off-line calculate control-parameter set $\{\mathbf{K}_1, \dots, \mathbf{K}_m\}$ for STATCOMs by solving established m optimization problems (20), which is aimed to ensure robust small-signal stability of subsystem $_{1,1} \sim$ subsystem $_{1,n}$ under m sub-conditions; 2) On-line adjust STATCOMs' control parameters based on real-time STATCOMs' reactive current outputs, IBRs' active power outputs and obtained

control-parameter set $\{\mathbf{K}_1, \dots, \mathbf{K}_m\}$, which assumes that real-time STATCOMs' reactive current outputs and IBRs' active power outputs can be obtained. The implementation procedure of this proposed adaptive control-parameter design method is shown in Fig. 3 with its main steps summarized as:

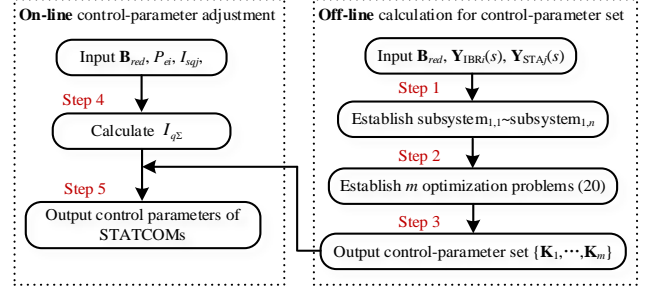


Fig. 3 Implementation procedure of proposed adaptive control parameter design method for STATCOMs.

1) In off-line process, establish subsystem $_{1,1} \sim$ subsystem $_{1,n}$ for the multi-IBR system with STATCOMs under *critical* operating conditions. If the inner parameters of IBRs are unknown, their internal dynamics can be identified by rational approximation based on frequency scan^[20];

2) Establish m optimization problems (20) to ensure small-signal stability of subsystem $_{1,1} \sim$ subsystem $_{1,n}$ under m sub-conditions, wherein m sub-conditions are obtained by dividing *critical* operating conditions. That is, $gSCR = \lambda_{\min}\{\mathbf{S}_B^{-1}\mathbf{B}_{redn}\}$ and $I_{q\Delta}$ is in m intervals, i.e., $[-1, -1+2/m], [-1+2/m, -1+4/m], \dots, [-1+2(m-1)/m, 1]$;

3) Output control-parameter set $\{\mathbf{K}_1, \dots, \mathbf{K}_m\}$ obtained by solving m optimization problems (20) through Matlab solvers;

4) In on-line process, calculate real-time reactive current output $I_{q\Delta}$ in (16) based on real-time IBRs' active power outputs and STATCOMs' reactive power outputs;

5) On-line adjust control parameters of STATCOMs based on control-parameter set $\{\mathbf{K}_1, \dots, \mathbf{K}_m\}$ and real-time $I_{q\Delta}$. To be specific, if $I_{q\Delta}$ is in interval $[-1+2(i-1)/m, -1+2i/m]$, then control parameters of all STATCOMs are set as \mathbf{K}_i .

VI. CASE STUDIES

In this section, the proposed grid-strength-based method and adaptive control method for a multi-IBR system with STATCOMs under varying operating conditions are validated by MATLAB/Simulink on a modified IEEE 39-node system as shown in Fig. 4, where nodes 1~9 are connected to IBRs through a set-up transformer, and node 39 is connected to external grids, simplified as an infinite bus. Each IBR represents a wind farm. IBRs' capacities refer to TABLE I. In practice, wind farms are commonly installed with a certain percentage of STATCOMs for voltage support. Due to this, we install 30%-capacity STATCOM for each IBR located at high-voltage side in the modified 39-node system as shown in Fig. 4. Network parameters refer to Ref. [21]. Control parameters of IBRs and STATCOMs refer to TABLES. II and III. Due to page limitation, we will focus on that IBRs have different configurations or control parameters in the following simulations. That IBRs are identical can be considered as a special case of a heterogeneous multi-IBR system.

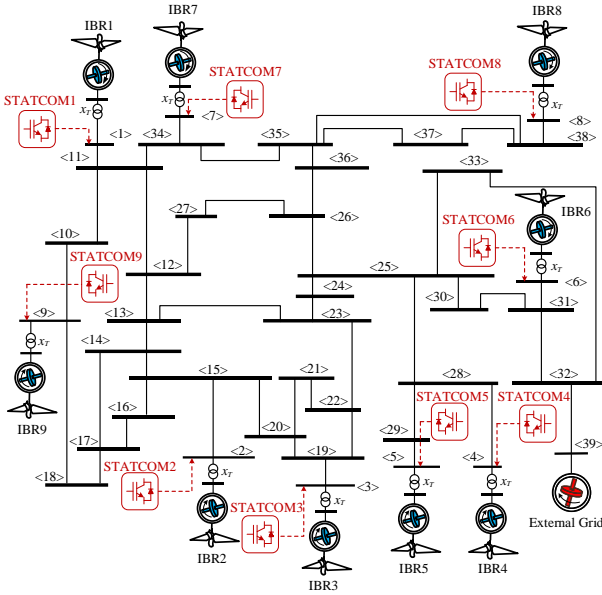


Fig. 4 A nine-IBR system with nine STATCOMs.

A. Verification of Theoretical Analysis in Sections III and IV

1) *Verification of proposed gSCR-based method.* As discussed in Section III, the theoretical analysis of STATCOMs' impact on system's stability is based on the proposed gSCR-based method. Due to this, we first verify the validity of proposed gSCR-based method by eigenvalue analysis in the modified 39-node system in Fig. 4. In this system, all STATCOMs are applied with the same AVC, but IBRs are heterogeneous: IBR1~IBR3 are applied with constant active power control, and the other IBRs are applied with dc voltage control, referring to TABLE II. Several cases are created by increasing active power outputs of all IBRs from 0.5 to 1 p.u at the same proportion, which are normalized at their rated capacities. The corresponding gSCR decreases from 3.36 to 1.68. Under these cases, we compare resulting dominant eigenvalues of the modified 39-node system and its *critical* subsystem, as shown in Fig. 5 (a). The corresponding loci of damping ratio of dominant eigenvalues for modified 39-node system is given in Fig. 5 (b) represented by red dotted curve.

It can be seen from Fig. 5 (a) that dominant eigenvalues of the *critical* subsystem match very well with the modified 39-node system, when gSCR is changed from 3.36 to 1.68. This indicates that small-signal stability of the multi-IBR system with STATCOMs can be represented by that of the *critical* subsystem under varying operating conditions.

Moreover, Fig. 5 (a) shows that gSCR can evaluate small-signal stability of the modified 39-node system under varying operating conditions, when control parameters of IBRs and STATCOMs are given. As shown in Fig. 5 (a), C_{gSCR} is equal to 2.1. When $gSCR = C_{gSCR}$, the system is critically stable; when $gSCR > C_{gSCR}$, the system is stable; besides, the larger ($gSCR - C_{gSCR}$) is, the more stable the system is; otherwise, if $gSCR < C_{gSCR}$, the system is unstable. The same conclusion can also be observed from the loci of damping ratio of the system in Fig. 5 (b). Simulation results are consistent with the theoretical analysis in Section III.

Furtherly, the electromagnetic time-domain simulation of the modified 39-node system is provided to verify the validity of the proposed gSCR-based method. When the active power outputs of all IBRs are set as 0.7 and 0.9 p.u., the corresponding gSCR are 2.404 and 1.87. Under these two cases, a disturbance is applied to the infinite bus at $t=1s$ to cause 0.05 p.u. voltage drop and lasts 0.05s. Time-domain responses of active power outputs of all IBRs under these two cases are given in Fig. 6.

It can be seen from Fig. 6 that when $gSCR=2.404 > 2.1$ (i.e., C_{gSCR} in Fig. 5), the system is stable. But when $gSCR=1.87 < C_{gSCR}$, the system is unstable. Time-domain simulation results are consistent with eigenvalue results from Fig. 5, which verifies the effectiveness of the proposed gSCR-based method.

TABLE I
RATED CAPACITIES OF EACH IBR (PER-UNIT)

IBR1	IBR2	IBR3	IBR4	IBR5
1	2	1	1	2
IBR6	IBR7	IBR8	IBR9	
10	2	2	1	

TABLE II
CONTROL PARAMETERS OF IBRS (PER-UNIT)

GFLCs	The PLL $H_{pll}(s)$	DC voltage loop $H_{dc}(s)$	Constant active power control loop $H_p(s)$
1~3	$16+9500/s$	/	$1+5/s$
4~6	$13+9800/s$	$0.5+5/s$	/
7~9	$16+9500/s$	$0.5+5/s$	/

Filter inductance L_f , filter capacitance C_f , dc capacitance C_{dc} : 0.05, 0.05, 0.038;
Transfer function of the current control loop $H_i(s)$: $1.5+10/s$;
Transfer function of the voltage feedforward control loop H_{ff} : $1/(1+0.0001s)$;
 q -axis current reference I_{qref} : 0.

TABLE III
CONTROL PARAMETERS OF STATCOMS (PER-UNIT)

Filter inductance L_{fs} , dc capacitance C_{dcs} : 0.1, 0.038;
Transfer function of current control loop $H_{is}(s)$: $1+10/s$;
Transfer function of dc voltage control loop $H_{dcs}(s)$: $1+5/s$;
Transfer function of the PLL $H_{plls}(s)$: $30+7000/s$;
Transfer function of the AVC $H_{avcs}(s)$: $1+5/s$

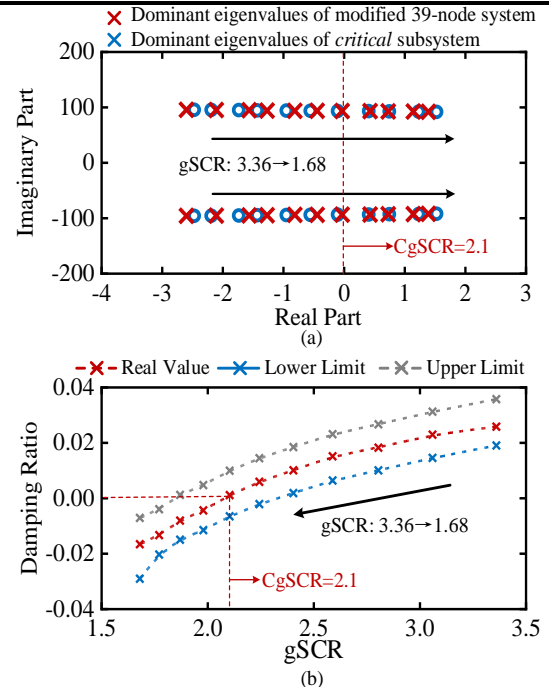


Fig. 5 when gSCR changes from 3.36 to 1.68: (a) Loci of dominant eigenvalues of modified 39-node system and *critical* subsystem; (b) Loci of damping ratio of dominant eigenvalues for modified 39-node system (red dotted curve), weakest subsystem (blue dotted curve) and strongest subsystem (grey dotted curve) in $subsystem_{1,1} \sim subsystem_{1,9}$.

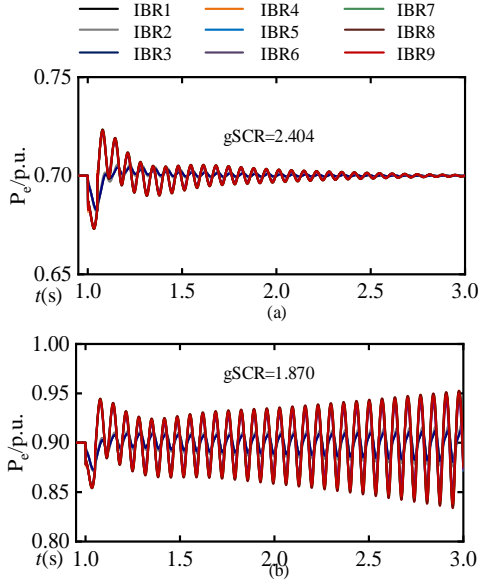


Fig. 6 Time-domain responses of active power outputs of IBR1~IBR9: (a) $gSCR=2.404$; (b) $gSCR=1.87$.

2) *Verification of STATCOMs' Impact Analysis.* As discussed in Section III.B, STATCOMs only influence $CgSCR$ under varying operating conditions. Besides, STATCOMs' impact on $CgSCR$ is uncertain, which depends on STATCOMs' dynamics. Here, we use the *critical* subsystem of the modified 39-node system (all IBRs output rated active power) to discuss how STATCOMs influence $CgSCR$. Five scenarios are considered:

- 1) Control parameters of STATCOM in the *critical* subsystem refer to TABLE III and $I_{q\Sigma}=-0.5$ p.u.;
- 2) Control parameters of STATCOM in the *critical* subsystem refer to TABLE III and $I_{q\Sigma}=0.5$ p.u.;
- 3) Control parameters of STATCOM in the *critical* subsystem refer to TABLE III, but PI parameters of AVC and PLL are set as "2.92, 5" and "10.3, 20000", and $I_{q\Sigma}=0.5$ p.u.;
- 4) Control parameters of STATCOM in the *critical* subsystem refer to TABLE III, $I_{q\Sigma}=0.5$ p.u., and $p_{\Sigma}=0.4$;
- 5) Disconnect STATCOM in the *critical* subsystem as a reference.

TABLE IV

$CgSCR$ OF CRITICAL SUBSYSTEM UNDER SCENARIOS 1)~5)

	Scenario 1)	Scenario 2)	Scenario 3)	Scenario 4)	Scenario 5)
p_{Σ}	0.3	0.3	0.3	0.4	0
$CgSCR$	1.31	2.24	1.28	2.3	1.94

TABLE IV shows $CgSCR$ of the *critical* subsystem under these five scenarios. According to Scenarios 1), 2) and 5), we can see that when $I_{q\Sigma}$ changes, STATCOM may increase (or decrease) $CgSCR$, i.e., deteriorate (or improve) system's stability. We can see from scenarios 2), 3) and 5) that when STATCOM's control parameters change, STATCOM may also increase (or decrease) $CgSCR$. These demonstrate that STATCOM's impact on $CgSCR$ is uncertain depending on STATCOM's dynamics, including control parameters and reactive current output. Besides, comparing scenarios 2), 4) and 5), we can see that the increase of p_{Σ} enlarges $CgSCR$. This indicates that p_{Σ} represents relative degree of STATCOM's

impact on $CgSCR$. Simulation results are consistent with theoretical analysis in Section III.B.

3) *Verification of Critical Operating Conditions.* As discussed in Section IV.A, when STATCOMs decrease $CgSCR$, under *critical* operating conditions that $gSCR=\lambda_{\min}\{S_B^{-1}B_{redn}\}$ in (8) and $I_{q\Sigma}$ in $[-1,1]$, the *critical* subsystem tends to be most unstable. This is because that when STATCOMs decrease $CgSCR$, the decrease of IBRs' active power output increases $gSCR$ but decreases $CgSCR$, resulting in the increase of $(gSCR-CgSCR)$. To verify *critical* operating conditions, we increase all IBRs' active power outputs in the modified 39-node system from 0.5 to 1 p.u. and set $I_{q\Sigma}$ of corresponding *critical* subsystem as a constant value -0.5 p.u.. The corresponding $gSCR$ changes from 3.36 to 1.68. Fig. 7 shows loci of dominant eigenvalues of corresponding *critical* subsystem. We can see from scenario 1) in TABLE IV that when $I_{q\Sigma}=-0.5$ p.u., STATCOMs decrease $CgSCR$. Besides, we can see from Fig. 7 that with the increase of IBRs' active power outputs and $I_{q\Sigma}=-0.5$ p.u., the system becomes more unstable. Simulation results are consistent with theoretical analysis.

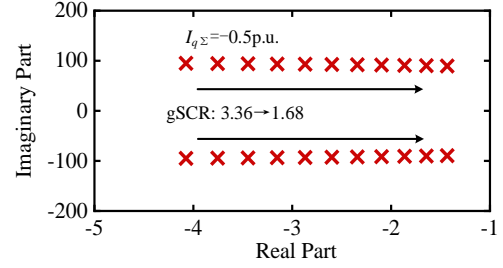


Fig. 7 Loci of dominant eigenvalues of the *critical* subsystem, when $gSCR$ changes from 3.36 to 1.68 and $I_{q\Sigma}=-0.5$ p.u..

4) *Verification that System's Stability is Bounded.* As discussed in Section IV.B, small-signal stability of the multi-IBR system with STATCOMs under varying operating conditions is bounded by that of subsystem_{1,1} and subsystem_{1,n}, which are corresponding to the most unstable and most stable subsystems. To verify this conclusion, we consider the scenarios in 1) of this subsection. Fig. 5 (b) shows the loci of damping ratios of subsystem_{1,1} and subsystem_{1,9} for the modified 39-node system, which are represented by blue and grey dotted curves. We can see from Fig. 5 (b) that the red dotted curve is between blue and grey dotted curves. This indicates that the modified 39-node system is bounded, which are consistent with theoretical analysis in Section IV.B.

B. Verification of Adaptive Control Parameter Design Method

The above subsection verifies that if STATCOMs decrease $CgSCR$, the system is most unstable under *critical* operating conditions; besides, small-signal stability of the multi-IBR system with STATCOMs under varying operating conditions is bounded by subsystem_{1,1}~subsystem_{1,n}. Therefore, the robust small-signal stability issues of the multi-IBR system with STATCOMs under varying operating conditions can be converted to that of subsystem_{1,1}~subsystem_{1,n} under *critical* operating conditions, with the pre-condition that STATCOMs decrease $CgSCR$. Here, we furtherly verify the validity of the

proposed adaptive control parameter design method for STATCOMs. Six cases are considered:

- 1) Divide *critical* operating conditions into 20 intervals;
- 2) Divide *critical* operating conditions into 10 intervals;
- 3) Divide *critical* operating conditions into 8 intervals;
- 4) Divide *critical* operating conditions into 4 intervals;
- 5) Divide *critical* operating conditions into 2 intervals;
- 6) Do not divide *critical* operating conditions.

Optimization problems (20) for cases 1)~6) are solved by Matlab solvers. The results for cases 1)~4) are given in TABLES. V~VIII in Appendix. But optimization problems (20) for cases 5)~6) have no solutions. This indicates that it may be hard to find fixed control parameters for STATCOMs to ensure robust small-signal stability of the multi-IBR system with STATCOMs under all operating conditions. Therefore, it is necessary to adaptively adjust STATCOMs' control parameters considering varying operating conditions.

Fig. 8 shows C_{gSCR} of the *critical* subsystem under *critical* operating conditions for cases 1)~4), and reference case that STATCOMs' control parameters refer to TABLE III but PLL's PI parameters are set as 22, 7300. Under these five cases, the system's C_{gSCR} is denoted as $C_{gSCR_{20}}$, $C_{gSCR_{10}}$, C_{gSCR_4} and C_{gSCR_0} , respectively. Besides, $gSCR$ and C_{gSCR} of modified 39-node system without STATCOMs under rated operating condition is 1.68 and 1.94.

As shown in Fig. 8, for the reference case, C_{gSCR} may be larger (or smaller) than 1.94, i.e., STATCOMs may deteriorate (or improve) system stability. Moreover, the increase of $I_{q\Sigma}$ may cause $C_{gSCR} > gSCR = 1.68$, i.e., the system becomes unstable. This demonstrates the necessity to dynamically adjust STATCOMs' control parameters to ensure robust small-signal stability of the multi-IBR system with STATCOMs under varying operating conditions. In comparison, C_{gSCR} of the *critical* subsystem under cases 1)~4) are always smaller than 1.5 (smaller than 1.68 and 1.94), when $I_{q\Sigma}$ is in range of $[-1, 1]$. That is, the obtained control parameters set for STATCOMs can ensure robust small-signal stability of the *critical* subsystem and that STATCOMs decrease C_{gSCR} of the *critical* subsystem under *critical* operating conditions. This illustrates that the proposed adaptive control parameter design method for STATCOMs can ensure robust small-signal stability of the multi-IBR system with STATCOMs under varying operating conditions. Besides, we can see that red and blue curves are commonly under brown and grey curves. This demonstrates that when the divided sub-conditions are more, the obtained STATCOMs' control-parameter set can improve the system's stability better.

Furtherly, the electromagnetic time-domain simulation of the modified 39-node system is provided to verify the proposed control method. Two operating conditions are considered: 1) all IBRs output rated active power and $I_{q\Sigma} = -0.241$ p.u.; 2) all IBRs output rated active power and $I_{q\Sigma} = 0.19$ p.u.. For each operating condition, we consider 5 scenarios:

- I) All STATCOMs use control parameters in TABLE V;
- II) All STATCOMs use control parameters in TABLE VI;
- III) All STATCOMs use control parameters in TABLE VII;
- IV) All STATCOMs use control parameters in TABLE VIII;

V) All STATCOMs use control parameters in TABLE III, but PLL's PI parameters are set as 22, 7300, as a reference.

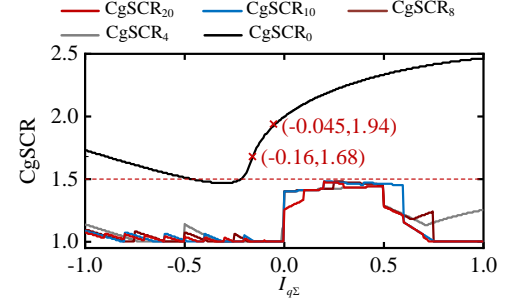


Fig. 8 C_{gSCR} for the *critical* subsystem under *critical* operating conditions for cases 1)~4) and the reference case that control parameters of STATCOMs refer to TABLE III, but PLL's PI parameters are 22, 7300.

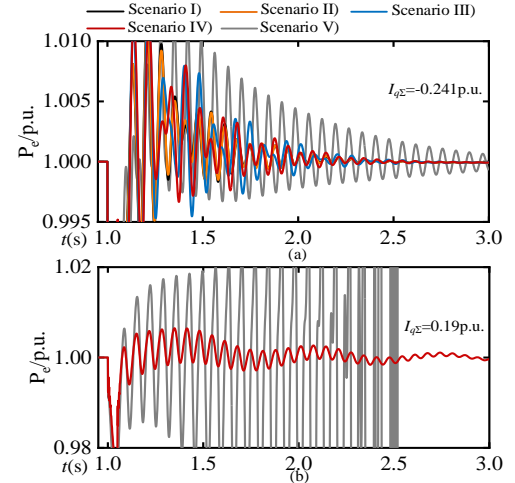


Fig. 9 Time-domain responses of IBR1's active power output under different scenarios for two operating conditions that all IBRs output rated active power: (a) $I_{q\Sigma} = -0.241$ p.u.; (b) $I_{q\Sigma} = 0.19$ p.u..

For each scenario, a disturbance is applied to infinite bus at $t=1$ s to cause 0.05 p.u. voltage drops and lasts 0.05s. Time-domain responses of active power outputs of IBR1 under these scenarios are given in Fig. 9. In Fig. 9 (b), since control parameters of STATCOMs in TABLE V~TABLE VIII in Appendix are the same when $I_{q\Sigma} = 0.19$ p.u., we only provide responses of IBR1's active power output under scenarios IV) and V). We can see from Fig. 9 that the system is robustly stable under different operating conditions, when STATCOMs use proposed adaptive control; but the system changes from stability to instability with fixed STATCOMs' control parameters, when $I_{q\Sigma}$ changes from -0.241 to 0.19 p.u.. Simulation results are consistent with the analysis by Fig. 8 and thus verify the validity of the proposed adaptive control parameter design method for STATCOMs.

VII. CONCLUSIONS

In this paper, an adaptive control-parameter design method for STATCOMs was proposed to ensure robust small-signal stability of a multi-IBR system with STATCOMs under varying operating conditions. Firstly, a grid-strength-based method was proposed to understand the impact mechanism of STATCOMs on IBR-induced oscillation issues considering varying operating conditions. Besides, based on this proposed method, we found *critical* operating conditions that the system

is most unstable; and the original system's stability is bounded by multiple subsystems. Due to this, we simplified the robust small-signal stability issues of the multi-IBR with STATCOMs under varying operating conditions as that of multiple subsystems under *critical* operating conditions, which can avoid traversing all operating conditions and modelling system's detailed dynamics. Moreover, an adaptive control-parameter design method is proposed for STATCOMs to ensure robust small-signal stability of the multiple subsystems under *critical* operating conditions. In the proposed control method, we calculated a control-parameter set for STATCOMs off-line, and on-line adjusted STATCOMs' control parameters through obtained control-parameter set, real-time STATCOMs' reactive current outputs and IBRs' active power outputs. The proposed control method can ensure the robust small-signal stability of the multi-IBR system with STATCOMs under varying operating conditions. The effectiveness of the proposed analysis method and control method were verified in a modified 39-node system. In our future works, we will explore how to coordinate IBRs and STATCOMs with other devices (e.g., energy storage devices and static var capacitors, SVC) to ensure the robust small-signal stability under varying operating conditions.

REFERENCES

- [1] Q. Peng, Q. Jiang, and et al., "On the stability of power electronics-dominated systems: challenges and potential solutions," *IEEE Trans. Ind. Appl.*, vol. 55, no. 6, pp. 7657-7670, Nov. 2019.
- [2] F. Milano, F. Dörfler, G. Hug, D. J. Hill, and G. Verbic, "Foundations and challenges of low-inertia systems," in *2018 Power Systems Computation Conference (PSCC)*. IEEE, pp. 1-25, 2018.
- [3] Y. Cheng, and et al., "Real-world subsynchronous oscillation events in power grids with high penetrations of inverter-based resources," *IEEE Trans. Power Systems*, vol. 38, no. 1, pp. 316-330, Jan. 2023.
- [4] H. Liu, X. Xie, and et al., "Subsynchronous interaction between direct-drive PMSG based wind farms and weak AC networks," *IEEE Trans. Power syst.*, vol. 32, no. 6, pp. 4708-4720, Nov. 2017.
- [5] J. Hu, B. Wang, and et al., "Small signal dynamics of DFIG-based wind turbines during riding through symmetrical faults in weak ac grid," *IEEE Trans. Energy Convers.*, vol. 32, no.2, pp. 720-730, Jun. 2017.
- [6] H. Zong, C. Zhang, X. Cai and M. Molinas, "Oscillation propagation analysis of hybrid AC/DC grids with high penetration renewables," *IEEE Trans. Power Syst.*, vol. 37, no. 6, pp. 4761-4772, Nov. 2022.
- [7] P. Sun, J. Yao, and et al., "Virtual capacitance control for improving dynamic stability of the DFIG-based wind turbines during a symmetrical fault in a weak ac grid," *IEEE Trans. Ind. Electron.*, vol. 68, no. 1, pp. 333-346, Jan. 2021.
- [8] D. Zhu, S. Zhou, X. Zou, and et al., "Small-signal disturbance compensation control for LCL-type grid-connected converter in weak grid," *IEEE Trans. Ind. Appl.* Vol. 56, no. 3, May, 2020.
- [9] Y. Zhu, Y. Gu, Y. Li and T. C. Green, "Participation analysis in impedance models: The grey-box approach for power system stability," *IEEE Trans. Power Syst.*, vol. 37, no. 1, pp. 343-353, Jan. 2022.
- [10] W. Du, Y. Wang, H. Wang, and et al., "Small-disturbance stability limit of a grid-connected wind farm with PMSGs in the timescale of DC voltage dynamics," *IEEE Trans. Power syst.*, vol. 36, no. 3, pp. 2366-2379, May. 2021.
- [11] Y. Zhang, Y. Yang, X. Chen, and et al., "Intelligent parameter design-based impedance optimization of STATCOM to mitigate resonance in wind farms," *IEEE J. Emerg. Sel. Topics Power Electron.*, vol. 9, no. 3, pp. 3201-3215, Jun. 2021.
- [12] H. Yuan, H. Xin, and et al., "Small-signal stability assessment of multi-converter-based-renewable systems with STATCOMs based on generalized short-circuit ratio," *IEEE Trans. Energy Convers.*, vol. 37, no. 4, pp. 2889-2902, Dec. 2022.

- [13] Y. Liao, X. Wang, "Impedance-based stability analysis for interconnected converter systems with open loop RHP poles," *IEEE Trans. Power Electron.*, vol. 35 no. 4, pp. 4388-4397, Apr. 2020.
- [14] L. Huang, and et al. "Grid-synchronization stability analysis and loop shaping for PLL-based power converters with different Reactive power control," *IEEE Trans. Smart Grid*, vol. 11, no. 1, pp. 501-516, Jan. 2020.
- [15] G. Li, Y. Chen, A. Luo and et. al., "An enhancing grid stiffness control strategy of STATCOM/BESS for damping sub-synchronous resonance in wind farm connected to weak grid," *IEEE Trans. Ind. Informat.*, vol. 16, no. 9, pp. 5835-5845, Sep. 2020.
- [16] P. Apkarian, D. Noll, "Nonsmooth H_∞ Synthesis," *IEEE Trans. Autom. Control*, vol. 51, no. 1, pp. 71-86, Jan. 2006.
- [17] Y. Zhou, G. Wang, et al., "Small-signal Stability Analysis of Power Systems under Uncertain Renewable Generation," *2022 IEEE Power & Energy Society General Meeting (PESGM)*, Denver, CO, USA, 2022.
- [18] H. Yuan, and et al., "Small Signal Stability Analysis of Grid-Following Inverter-Based Resources in Weak Grids With SVGs Based on Grid Strength Assessment," *2021 IEEE 1st International Power Electronics and Application Symposium (PEAS)*, Shanghai, China, 2021.
- [19] H. Liang, et al., "Optimal Capacity Allocation of Renewable Energy Generation Base for Small Signal Stability Improvement," *2019 IEEE Innovative Smart Grid Technologies - Asia (ISGT Asia)*, Chengdu, China, 2019, pp. 1772-1776.
- [20] B. Gustavsen and A. Semlyen, "Rational approximation of frequency domain responses by vector fitting," *IEEE Transactions on Power Delivery*, vol. 14, no. 3, pp. 1052-1061, 1999.
- [21] L. Huang, H. Xin, W. Dong, and F. Dörfler, "Impacts of grid structure on PLL-synchronization stability of converter-integrated power systems," arXiv preprint arXiv:1903.05489, 2019.

APPENDIX

TABLE V

OPTIMAL CONTROL-PARAMETER SET FOR STATCOMS UNDER CASE 1)					
$I_{q\bar{z}}$	[-1, -0.9]	[-0.9, -0.8]	[-0.8, -0.7]	[-0.7, -0.6]	[-0.6, -0.5]
PLL	30.6+5796.4/s	28.5+5857.9/s	26.5+5915.0/s	24.4+5966.5/s	22.3+6009.7/s
AVC	2.75+5/s	2.77+5/s	2.79+5/s	2.81+5/s	2.83+5/s
$I_{q\bar{z}}$	[-0.5, -0.4]	[-0.4, -0.3]	[-0.3, -0.2]	[-0.2, -0.1]	[-0.1, 0]
PLL	20.2+6040.5/s	18+6053.7/s	15.5+6020/s	12.8+6020/s	9.6+5547.3/s
AVC	2.85+5/s	2.88+5/s	2.91+5/s	2.91+5/s	2.98+5/s
$I_{q\bar{z}}$	[0, 0.1]	[0.1, 0.2]	[0.2, 0.3]	[0.3, 0.4]	[0.4, 0.5]
PLL	5.1+3974.1/s	1+100/s	119.6+100/s	1+100/s	1+100/s
AVC	3.01+5/s	3.02+5/s	3.02+5/s	3.01+5/s	3.01+5/s
$I_{q\bar{z}}$	[0.5, 0.6]	[0.6, 0.7]	[0.7, 0.8]	[0.8, 0.9]	[0.9, 1]
PLL	10.3+20000/s	9.2+14771.8/s	10+13302.9/s	11+12837.2/s	12.1+12582.9/s
AVC	2.93+5/s	2.86+5/s	2.79+5/s	2.71+5/s	2.64+5/s

TABLE VI

OPTIMAL CONTROL-PARAMETER SET FOR STATCOMS UNDER CASE 2)					
$I_{q\bar{z}}$	[-1, -0.8]	[-0.8, -0.6]	[-0.6, -0.4]	[-0.4, -0.2]	[-0.2, 0]
PLL	29.5+5791.6/s	25.3+5902.2/s	21+5974.7/s	16.3+5942.2/s	10.2+5381.8/s
AVC	2.79+5/s	2.82+5/s	2.86+5/s	2.92+5/s	2.99+5/s
$I_{q\bar{z}}$	[0, 0.2]	[0.2, 0.4]	[0.4, 0.6]	[0.6, 0.8]	[0.8, 1]
PLL	1+100/s	119.6+100/s	97.8+100/s	9.2+14726.5/s	11.1+12831.5/s
AVC	3.02+5/s	3+5/s	2.97+5/s	2.85+5/s	2.7+5/s

TABLE VII

OPTIMAL CONTROL-PARAMETER SET FOR STATCOMS UNDER CASE 3)					
$I_{q\bar{z}}$	[-1, -0.75]	[-0.75, -0.5]	[-0.5, -0.25]	[-0.25, 0]	[0, 0.25]
PLL	28.9+5785.7/s	23.6+5909.5/s	17.9+5927.3/s	10.5+5316.3/s	1+100/s
AVC	2.8+5/s	2.84+5/s	2.91+5/s	2.99+5/s	3.02+5/s
$I_{q\bar{z}}$	[0.25, 0.5]	[0.5, 0.75]	[0.75, 1]		
PLL	105.2+100/s	10.3+20000/s	10.5+13036/s		
AVC	2.98+5/s	2.92+5/s	2.74+5/s		

TABLE VIII

OPTIMAL CONTROL-PARAMETER SET FOR STATCOMS UNDER CASE 4)					
$I_{q\bar{z}}$	[-1, -0.5]	[-0.5, 0]	[0, 0.5]	[0.5, 1]	
PLL	25.8+5701.1/s	12.2+4900.7/s	1+100/s	10.9+20000/s	
AVC	2.87+5/s	3+5/s	3.02+5/s	2.9+5/s	